



# The significance of soil-foundation compliance on the dynamic identification of the Chiaravalle viaduct

Sandro Carbonari<sup>a</sup>, Francesca Dezi<sup>b</sup>, Fabrizio Gara<sup>a</sup>, Graziano Leoni<sup>c</sup>

<sup>a</sup> Department of Construction, Civil Engineering and Architecture, Università Politecnica delle Marche, Via Brecce Bianche, 60131 Ancona, Italy

<sup>b</sup> Department of Economics, Sciences and Law, University of San Marino, Contrada Omerelli, 47890 Republic of San Marino

<sup>c</sup> School of Architecture and Design, Università di Camerino, Viale della Rimembranza, 63100 Ascoli Piceno, Italy

*Keywords: Ambient vibration tests, dynamic identification, soil-foundation compliance, soil-structure interaction*

## ABSTRACT

The paper addresses the significance of soil-structure interaction on the dynamic behaviour of the “Chiaravalle viaduct”, based on ambient vibration measurements and numerical simulations through a finite element model. The viaduct is located in Central Italy and is founded on piles in an eluvial-colluvial soil deposit. Experimental modal properties are evaluated by means of the operational modal analysis on accelerometric data, and the role of soil-structure interaction in the interpretation of tests is identified by means of a refined finite element model of the viaduct. In the soil-structure interaction models the local site conditions in correspondence of each bridge pier (resulting from geotechnical and geophysical investigations) are taken into account in the definition of the soil-foundations impedances. Comparisons between the experimental and numerical results highlight the role of the pile-soil-pile interaction, the radiation problem, the pile cap embedment and the variability of the soil stratigraphy along the longitudinal direction of the viaduct in the interpretation of the experimental data.

## 1 INTRODUCTION

The high Italian seismicity in conjunction with the existing dense transport infrastructure network require the seismic verification and upgrading of key components of the network links, especially bridges, to improve the overall earthquake resilience of communities. In this framework, system identification and structural health monitoring of structures have recently drawn attention for developing assessment tools and reducing uncertainties in the risk assessment procedures. Estimation of the dynamic properties of bridges using recorded vibration data allows the calibration of numerical models for the assessment of the structural safety and for the design of a seismic retrofit (e.g. Omenzetter et al., 2013; Zonta et al., 2014). The Ambient Vibration Test (AVT) is one of the most attractive methods for the evaluation of the dynamic properties of existing constructions in elastic range since it uses natural vibrations as input and foresees the use of small and portable instrumentation. It is

generally common practice to perform AVTs, to get modal parameters through the Operational Modal Analysis (OMA) (Overschee and De Moor, 1996; Dohler et al., 2010) and then to calibrate finite element models by changing the mechanical properties of materials, achieving the best fit of the model results with the experimental data. On the contrary, geometry of structural components is assumed in a deterministic way and the structure is assumed to be fixed at the base. However, it is well-known in the literature, from both numerical (e.g. Capatti et al., 2017; Dezi et al., 2012; Carbonari et al., 2011; Kappos et al., 2002; Sextos et al., 2003) and experimental studies (e.g. Trifunac et al., 2001; Faraonis et al., 2015), that Soil-Structure Interaction (SSI) may play an important role in the dynamic structural response, especially for medium or soft soil conditions and for existing bridges. Thus, numerical models developed to interpret results of vibrational measurements should include the soil-foundation compliance.

This paper addresses the significance of soil-structure interaction in the interpretation of AVTs performed on the Chiaravalle viaduct, for which

detailed experimental campaigns and surveys on both the soil deposit and the superstructure are available. A 3D finite element model of the bridge is developed accounting for the soil-foundation compliance through Lumped Parameter Models (LPMs) (Carbonari et al., 2018) reproducing the dynamic impedances of soil-foundation systems. The latter are obtained with a refined 3D solid model accounting for the pile-soil-pile interaction, the radiation problem and the pile cap embedment. Modal parameters obtained from the OMA are compared with those derived from the numerical models of the bridge.

## 2 THE CHIARAVALLE VIADUCT

The Chiaravalle Viaduct in Central Italy connects the SS76 road to the Raffaello Sanzio airport (Figure 1a). The viaduct has a total length of 875 m and is constituted by 4 Kinematic Chains (KC#), separated by structural joints. The KCs, of 13, 10, 3 and 5 spans, respectively, each one of length 27.5 m, are constituted by simply supported girders connected over the piers through post-tensioned cables at the level of the concrete slab. The deck is 12.10 m wide and is constituted by three simply supported V-shaped r.c. beams underlying a 0.25 m thick concrete slab. The column bent piers are constituted by 2 circular columns with diameter of 1.4 m, with heights ranging between 6÷12 m. Only pier P17 of KC2 is characterized by a single column with a rounded rectangular cross section (Figure 1a). Piers foundation is constituted by 6 r.c. piles of length 30 m and diameter 1 m, connected by a rigid cap of dimensions 5 x 9 x 1.70 m (Figure 1b). During construction, 240 concrete samples were tested; results, in conjunction with tests performed for the retrofit design, allow to assume the mechanical parameters (mean compressive strength  $f_{cm}$  and elastic modulus  $E_{cm}$ ) reported in Table 1. Rebars FeB44k with nominal yielding strength of 435 MPa were used.

From the geomorphological point of view, the viaduct is located in a wide almost flat area with low altitudes set at almost 17-20 m above the mean sea level. With reference to Figure 2a, the geological configuration of the site is constituted by three main formations: a Plio-Pleistocene marine deposit, prevalently composed of Pleistocene marly, silty clays (AD4) underlying a recent continental covering soil that mainly consists of Quaternary (Pleistocene-Holocene) eluvial-colluvial (sandy and clayey silts, AD1) and Plio-Pleistocene alluvial (mainly sandy

gravels with clayey silts lenses, AD2) deposits. Locally, above the Plio-Pleistocene clayey substratum, lenses of sands in clayey-silty matrix can be found (AD3). The area was investigated by means of Boreholes (B), laboratory tests (e.g. triaxial tests, oedometer test) and in-situ Standard Penetration Test (SPT) conducted up to a maximum depth of about 24 m. The geophysical characterization was performed through a Multichannel Analysis of Surface Waves (MASW) and Down Holes (DH). Locations of tests are shown in Figure 2a, b. Furthermore, two Piezometers (PZ) were used to monitor the ground-water level along the viaduct. Results of surveys leads to the mechanical and dynamic parameters reported in Table 2 for each lithotype.

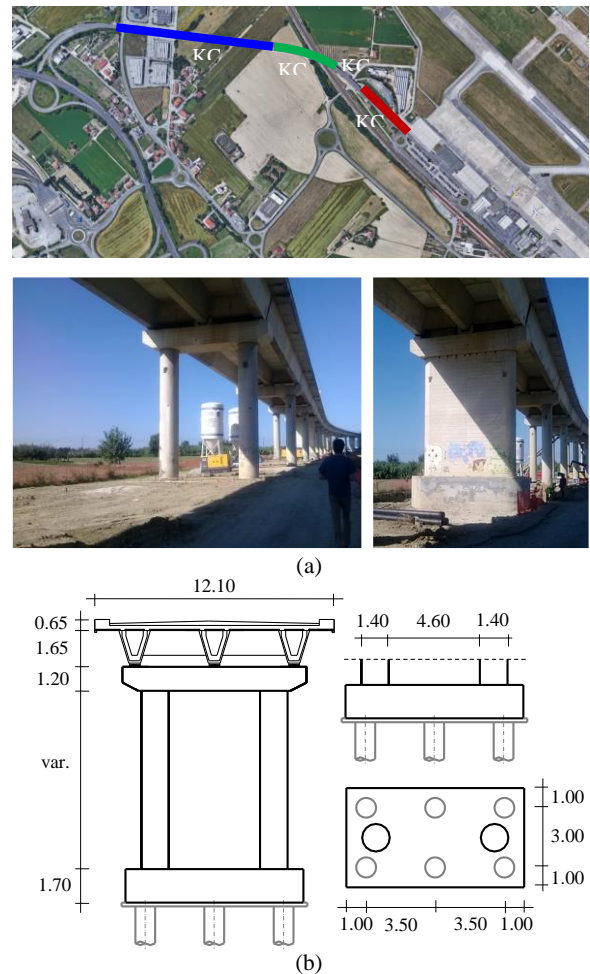


Figure 1. (a) Plan location of KCs and view of the viaduct, (b) pier elevation and foundations in [m].

Table 1. Mechanical properties of concrete.

Structural element	n. of specimens	$f_{cm}$ [MPa]	$E_{cm}$ [MPa]
Columns	33	17.0	25796
Foundation piles	20	7.5	20181
Pile caps	29	12.8	23691
Column bent	8	27.1	29670
Beams	10	40.7	33520

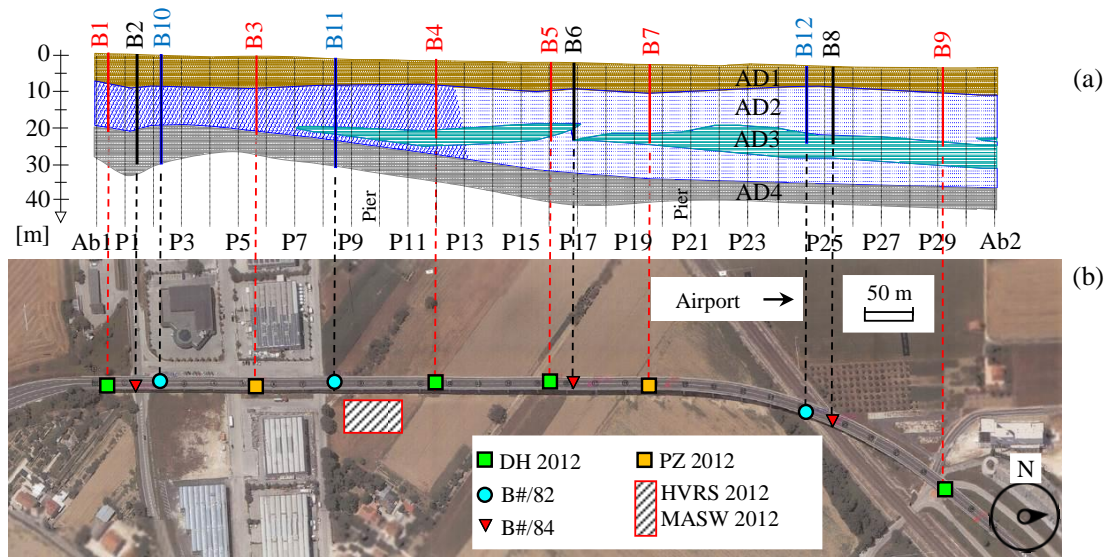


Figure 2. (a) Soil geological profile, (b) position of the test site and geotechnical surveys.

Table 2. Mechanical and dynamic parameters

Soil	$\gamma$ [kN/m <sup>3</sup> ]	$I_D$ [%]	$c'$ [kPa]	$c_u$ [kPa]	$\Phi'$ [°]	$E_s$ [kPa]	$E_{oed}$ [kPa]	$V_s$ [m/s]	$G_0$ [kPa]
AD1	19.02	-	20	20	27	63000	8700	230	92000
AD2	19.60	63	-	-	39	42000	-	540	567000
AD3	20.00	-	7	35	27	15000	-	325	218000
AD4	20.00	-	30	400	26	70000	-	600	770000

$I_D$  = density index       $V_s$  = shear wave velocity       $c'$  = drained cohesion  
 $\gamma$  = unit weight of soil       $G_0$  = small strain shear modulus       $c_u$  = undrained cohesion  
 $\Phi'$  = angle of internal friction       $E_s$  = elastic modulus       $E_{oed}$  = oedometric modulus

### 3 AMBIENT VIBRATION TESTS

Ambient vibration measurements were performed to evaluate modal parameters of the viaduct to develop and validate a finite element model for the design of the bridge seismic upgrading. AVTs are carried out with low noise unidirectional piezoelectric accelerometers connected to a 24-bit data acquisition system by means of coaxial cables and a portable PC for data storage. Each KC is monitored separately, and different sensor configurations are scheduled where necessary to cover the overall length of the KC, due to the limited availability of sensors. KC3 was not investigated due to logistic problems. Tests for each KC were performed in different days during the same week of July 2014 in the same timeslot so that ambient effects on the estimated modal parameters can be considered negligible (e.g. Regni et al., 2018; Xu et al., 2010; Xia et al., 2012).

In order to catch the transverse dynamic behaviour of the bridge, unidirectional accelerometers are placed at each span support and

oriented in the transverse direction. For each configuration, 1800 seconds long records sampled at a rate of 2048 Hz are acquired. All the recorded data are processed with standard signal processing techniques before performing the modal analyses. Initially, data are inspected to eliminate anomalous behaviours (signal clipping, intermittent noise, spikes and so on); then, the contribution of spurious trends is eliminated through a baseline correction and the high frequency content is eliminated by filtering (cut-off frequency of 20 Hz). Finally, signals are down-sampled at 51.2 Hz to decrease the number of data. The Covariance driven Stochastic Subspace Identification method (SSI-Cov) technique was used to identify the dynamic properties of the viaduct (Overschee and De Moor, 1996).

### 4 NUMERICAL MODELLING STRATEGY FOR THE AVTS INTERPRETATION

A refined 3D finite element model of the Chiaravalle viaduct is developed to interpret results of AVTs. As for the superstructure, both



the deck and the column bent piers are modelled with elastic frame elements taking into account the real position of the elements centroids through the use of rigid links. Mechanical properties of the concrete are based on experimental results presented in Table 1. At the abutments and piers positions, bridge supports are modelled through elastic links reproducing stiffnesses of elastomeric bearings. A Fixed Base model (FB) as well as a Compliant Base model (CB) of the viaduct, accounting for the soil-foundation dynamic stiffnesses are developed. In Figure 3a some pictorial views of the FB model are reported.

The CB model, addressing the SSI problem, is developed in the framework of the substructure approach, which allows analysing separately the soil-foundation and the superstructure systems. The analysis of the soil-foundation subdomain furnishes the frequency-dependent complex dynamic impedance matrix of the system that represents the behaviour of the superstructure restraints. Since software dedicated to structural modelling generally performs time domain analyses, the frequency dependent behaviour of the soil-foundation system is generally included through the use of LPMs constituted by assemblages of frequency independent springs, dashpots and masses. Parameters of the lumped system are calibrated in order to assure the best match between its dynamic stiffness matrix and that of the actual soil-foundation system in a selected frequency range. The LPM presented by Carbonari et al. (2018) is adopted to simulate the soil-foundation dynamic behaviour of each pier in the CB model (Figure 3b).

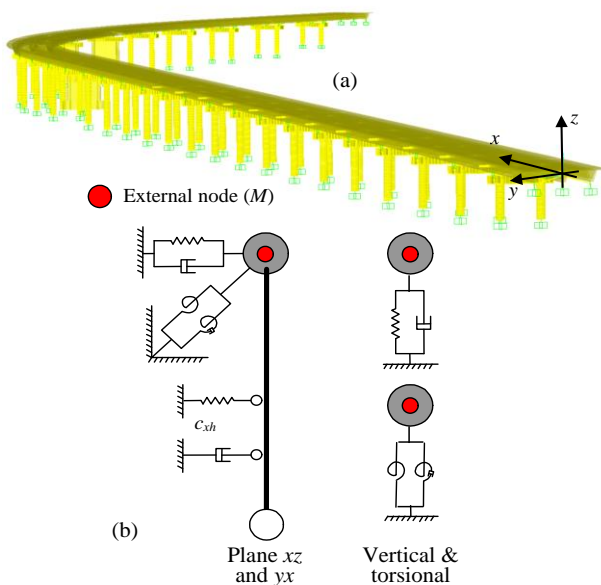


Figure 3. (a) Fixed base model (FB), (b) adopted LPM.

Each LPM is characterized by 24 parameters and is able to reproduce the frequency dependent translational, rotational and coupled roto-translational dynamic behaviour of the pile foundations characterised by a double symmetric layout. The external node, representing the interface between the soil-foundation system and the superstructure, is located at the intersection of the two symmetry axes.

#### 4.1 Soil-foundation modelling

The analysis of the soil-foundation system necessary to determine the relevant frequency-dependent impedance matrix is performed adopting a refined 3D solid model. Taking into account the 2D stratigraphic profile, characterised by an almost constant thicknesses of soil layers for the first 20 m, only one soil-foundation system, assumed to be representative for all the bridge, is developed.

The numerical model is developed within the computer software ANSYS. 8-node brick elements with linear interpolation functions are used to model a cylindrical soil portion with diameter  $D$  and height  $T$  satisfying conditions  $D/d = 50$  and  $T/d = 45$  (Figure 4) where  $d$  is the pile diameter. The soil is assumed to be a viscoelastic material and infinite elements are provided at boundaries to absorb the outgoing waves and to satisfy the radiation condition.

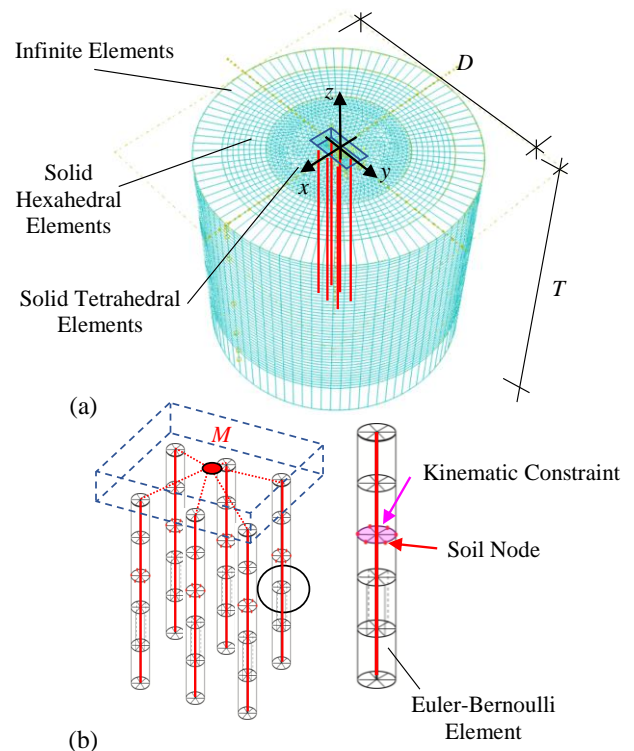


Figure 4. 3D solid finite element model of the soil-foundation system.

Piles are modelled with 2-node beam elements and their physical dimensions are taken into account by removing cylinders of soils. The beam-solid coupling is assured exploiting potentials of the software.

The pile cap, which is assumed to be rigid, is simulated through the soil excavation and the introduction of a rigid constraint between soil-cap interfaces and the piles head with master node  $M$ . Meshing criteria aim at obtaining an as much as possible structured mesh and at assuring a sufficient number of nodes per wavelength. Some validation studies are preliminarily performed to define the mesh dimension balancing results reliability with computational efforts; in particular, the mesh dimension is selected so as the propagation of waves with frequency up to 10 Hz is well captured. Components of the impedance matrix are obtained by imposing unit steady harmonic displacements at the fully restrained master node and evaluating the relevant reaction forces.

Figure 5 shows impedances obtained from the 3D solid model. A change of the impedance functions slopes at 9.2 Hz is evident; the latter is due to the cut-off frequency of the deposit associated to the fundamental vibration mode of the first soil layer (lithotype DA1) that is characterised by a very low shear modulus with respect to the underlying lithotypes. However, as will be shown later, results of experimental tests

(AVTs) revealed that the first three structural fundamental frequencies, which are expected to dominate the transverse dynamic response of the bridge, fall below 5 Hz. For this reason, parameters of LPMs are calibrated to reproduce the soil-foundation impedances in the frequency range 0-8 Hz. Impedances of the LPM are reported in Figure 5 with dotted lines. The lumped model is able to capture the dynamic behaviour of the comprehensive 3D solid model very well.

## 5 EXPERIMENTAL VS NUMERICAL RESULTS

In this section results of AVTs are presented in terms of fundamental structural frequencies, modal damping ratios and mode shapes, providing comparisons with those obtained from the developed numerical models (FB and CB).

Figure 6a shows for each KC the normalised mean amplitude of transverse displacements measured above piers at the deck level, obtained from the steady-state analysis of the CB model. For each KC, the highest amplitude peaks are evident in correspondence of the relevant chain fundamental frequencies; in addition, the interaction of the  $i$ -th KC is revealed by the presence of lower response peaks also in the response of the other KCs.

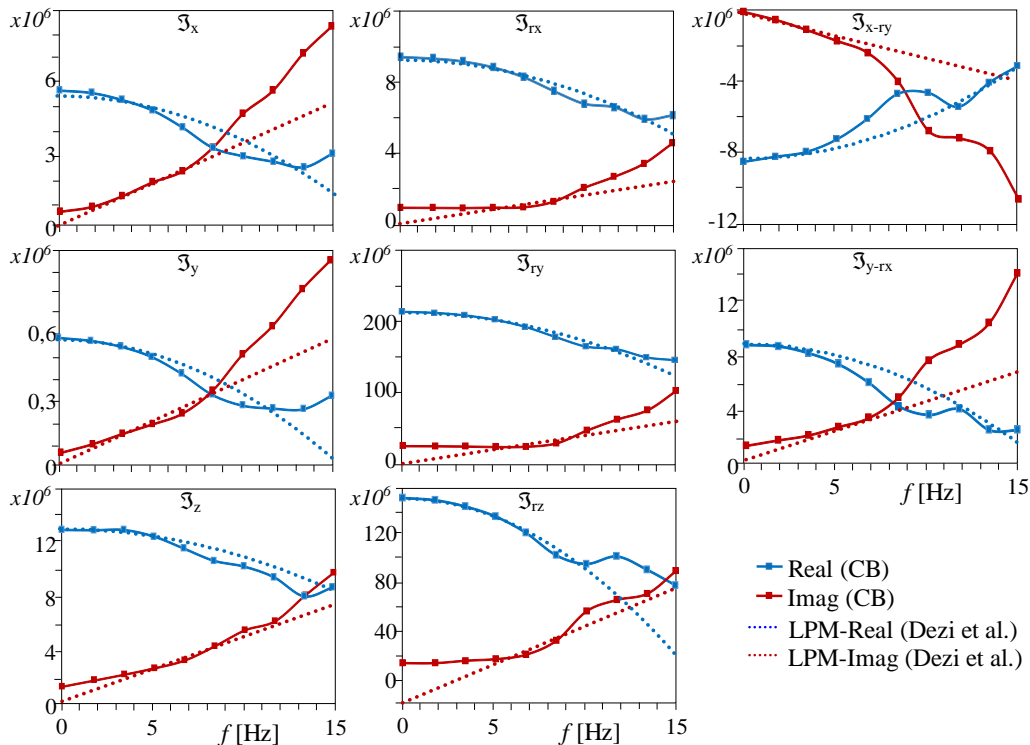


Figure 5. Comparison of foundation impedances for the CB-P and CB-P&C models.

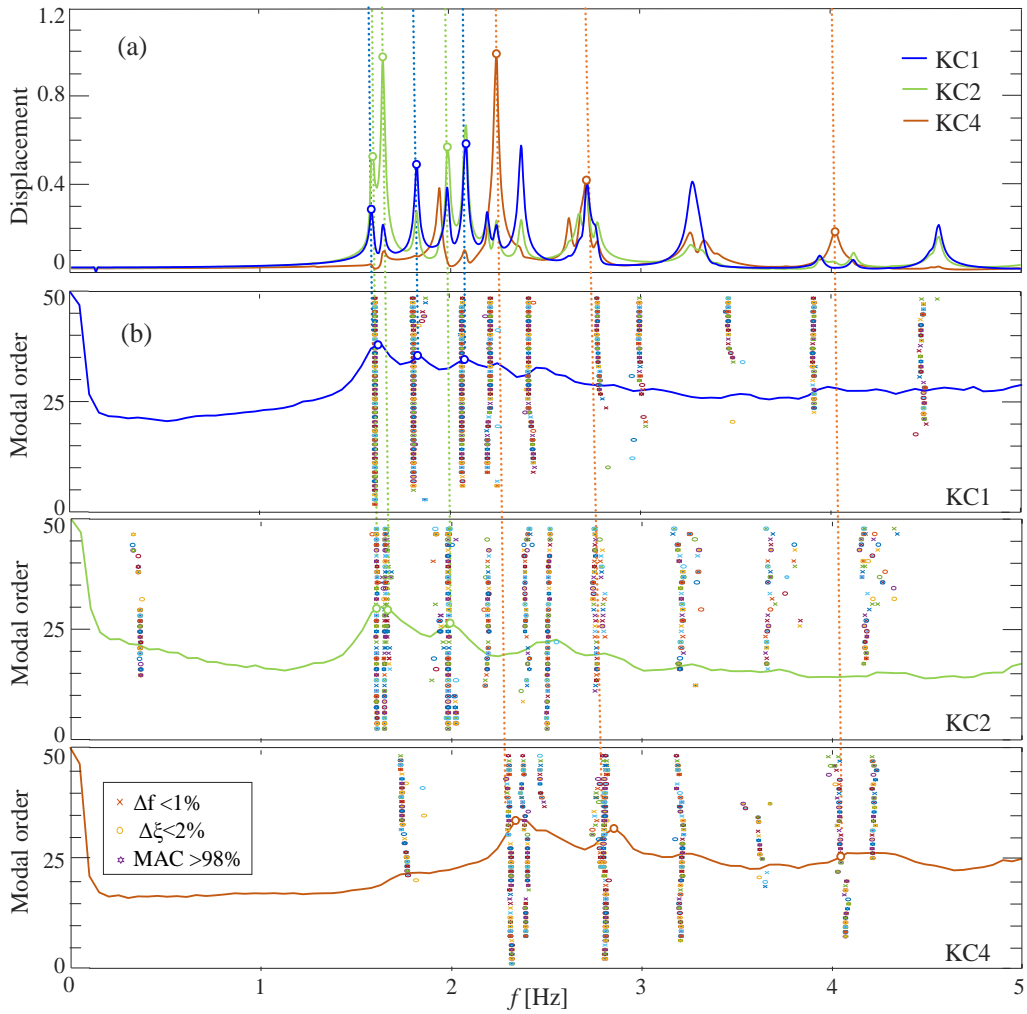


Figure 6. (a) Mean displacement amplitudes from the CB model, (b) stabilization diagrams.

Three fundamental frequencies are highlighted in Figure 6a for each KC, referred to as mode 1, 2 and 3 of the relevant KC for the sake of simplicity; these will be used in to compare experimental and numerical mode shapes.

Figure 6b shows the stabilization diagrams obtained from the OMA (continuous lines are the average of PSD of sensors positioned on the KCs), used to identify the viaduct fundamental frequencies. It can be observed that the experimental response is consistent with the numerical one: in particular, peaks in the stabilization diagrams are almost aligned with the numerical ones for each KC, as highlighted by vertical dotted lines (different colours are used for the KCs). Furthermore, also the measured relative amplitude of peaks at different frequencies is almost reproduced by the numerical model for all the KCs, with minor differences for what concern the first peaks of KC1. Results from the FB model is not reported in Figure 6a since its response is sensibly different from the measured one.

Results from FB model are presented in terms

of frequencies and mode shapes. It is worth mentioning that frequencies and mode shapes of the CB model are determined from steady-state analyses while modal analysis are used for the FB model, which is classically damped.

Table 3 compares the selected three fundamental structural frequencies obtained from the AVTs through the OMA and from the developed numerical models. With reference to experimental results, values of damping ratios are also reported for completeness. It can be observed that frequencies resulting from the FB model are sensibly higher than the experimental ones; thus, the model appear not able to capture the actual viaduct dynamic behaviour. The CB model better reproduces the experimental data with relative errors always below 1% (excepting mode 3 of KC2).

Figure 7 compares the three transverse mode shapes previously selected for KC1, KC2 and KC4, obtained from the experimental tests and the numerical models, normalised with respect to its relevant maximum transverse displacement.

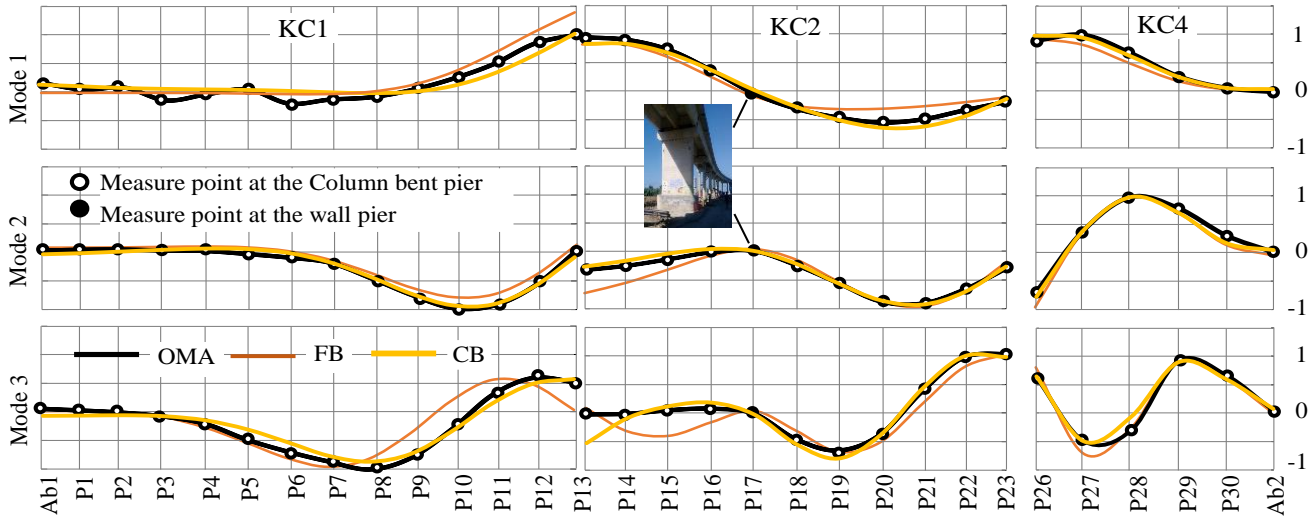


Figure 7. Comparison of numerical and experimental mode shapes.

Table 3. Comparison of experimental and numerical fundamental frequencies.

KC #	Mode	OMA		CB-P&C		FB	
		$f$ [Hz]	$\xi$ (-)	$f$ [Hz]	$\Delta f$ (%)	$f$ [Hz]	$\Delta f$ (%)
1	1	<b>1.61</b>	0.57	1.60	-0.6	1.71	5.8
	2	<b>1.81</b>	1.91	1.83	1.1	1.87	3.2
	3	<b>2.05</b>	1.78	2.08	1.4	2.14	4.2
2	1	<b>1.58</b>	0.93	1.59	0.6	1.62	2.5
	2	<b>1.66</b>	0.43	1.66	0.0	1.71	2.9
	3	<b>1.98</b>	0.60	2.03	2.5	2.14	7.5
4	1	<b>2.26</b>	0.42	2.26	0.0	2.41	6.2
	2	<b>2.79</b>	0.27	2.79	0.0	2.84	1.8
	3	<b>4.04</b>	0.21	4.04	0.0	4.28	5.6

Experimental data are reported with dots connected with black lines while continuous lines are used for the results of the numerical models. With reference to the CB model, it can be observed that numerical and experimental mode shapes are practically superimposed, with slight differences in the case of mode 2 of KC2. On the contrary, the FB model is not able to interpret all the experimental mode shapes.

## 6 CONCLUSIONS

The significance of soil-structure interaction in the interpretation of vibrational tests performed on bridges has been discussed in this work, with reference to a multi-span r.c. viaduct in Central Italy for which detailed experimental campaigns and surveys on both the soil deposit and the superstructure were available for the need of a

seismic upgrading of the structure. Ambient vibration measurements are performed on the superstructure to validate a finite element model of the viaduct for the seismic upgrading design. A conventional fixed base, as well as a numerical model accounting for the soil-foundation compliance, are developed to interpret the experimental data. The soil-structure interaction is included through the substructure approach, simulating the frequency-dependent soil-foundation impedances through lumped parameter models. Models accuracy in reproducing the experimental modal parameters is evaluated on the basis of both fundamental frequencies and mode shapes. It is found that a numerical model addressing the soil-structure interaction problem in a comprehensive way, i.e. including both the pile-soil-pile and pile-cap interactions, is necessary to correctly interpret the experimental data.

Overall, the presented case study demonstrates that the common practice of calibrating and updating fixed base numerical finite element models to fit experimental results from ambient vibration tests by only changing mechanical properties of materials should be prudently evaluated in the case of bridges, for which soil-structure interaction effects may significantly affect the structure dynamics, especially in the case of soft or medium soil deposits.

## REFERENCES

- Omenzetter, P., Beskhyroun, S., Shabbir, F., Chen, G.W., Chen, X., Wang, S., Zha, A., 2013. Forced and ambient vibration testing of full scale bridges. A report

- submitted to Earthquake Commission Re-research Foundation (Project No. UNI/578).
- Zonta, D., Glisic, B., Adriaenssens, S., 2014. Value of information: impact of monitoring on decision-making. *Struct. Control Health Monit.* **21**, 1043–1056.
- Capatti, M.C., Tropeano, G., Morici, M., Carbonari, S., Dezi, F., Leoni, G., Silvestri, F., 2017. Implications of non-synchronous excitation induced by nonlinear site amplification and soil-structure interaction on the seismic response of multi-span bridges founded on piles. *Bulletin of Earthq. Enging.*, **15**(11), 4963-4995.
- Carbonari, S., Morici, M., Dezi, F., Gara, F., Leoni, G., 2017. Soil-structure interaction effects in single bridge piers founded on inclined pile groups. *Soil Dyn. and Earthq. Enging.*, **92**, 52-67.
- Dezi, F., Carbonari, S., Tombari, A., Leoni, G., 2012. Soil-structure interaction in the seismic response of an isolated three-span motorway overcrossing founded on piles. *Soil Dyn. and Earthq. Enging.*, **41**, 151-163.
- Carbonari, S., Dezi, F., Leoni, G., 2011. Seismic soil-structure interaction in multi-span bridges: application to a railway bridge. *Earthq. Enging. and Struct. Dyn.*, **40**(11), 1219-1239.
- Kappos, A.J., Manolis, G.D., Moschonas, I.F., 2002. Seismic assessment and design of R/C bridges with irregular configuration, including SSI effects. *Intern. J. of Enging. Struct.*, **24**(10), 1337–48.
- Sextos, A.G., Pitilakis, K.D., Kappos, A.J., 2003. Inelastic dynamic analysis of RC bridges accounting for spatial variability of ground motion, site effects and soil-structure interaction phenomena. Part 2: Parametric study. *Earthq. Enging. and Struct. Dyn.*, **32**(4), 629-52.
- Trifunac, M.D., Todorovska, M.I., Hao, T.Y., 2001. Full-Scale experimental studies of soil-structure interaction. *Proc. 2nd U.S. - Japan Workshop on Soil-Structure Interaction*, Tsukuba City, Japan.
- Faraonis, P., Sextos, A., Chatzi, E., Zabel, V. Model updating of a bridge-foundation - soil system based on ambient vibration data. *UNCECOMP 2015, 1st ECCOMAS Thematic Conference on International Conference on Uncertainty Quantification in Computational Sciences and Engineering*, Papadrakakis M, Papadopoulos V, Stefanou G (eds.) Crete Island, Greece, 25–27 May 2015.
- Carbonari, S., Morici, M., Dezi, F., Leoni, G., 2018. A Lumped Parameter Model for Time-Domain Inertial Soil-Structure Interaction Analysis of Structures on Pile Foundations. *Earthq. Enging. and Struct. Dyn.*, **47**(11), 2147-2171.
- Regni, M., Arezzo, D., Carbonari, S., Gara, F., Zonta, D., 2018. Effect of Environmental Conditions on the Modal Response of a 10-Story Reinforced Concrete Tower. *Shock and Vibrations*, Article ID 9476146.
- Xu, Y.L., Chen, B., Ng, C.L. et al., 2010. Monitoring temperature effect on a long suspension bridge. *Struct. Control Health Monit.*, **17**, 632-653.
- Xia, Y., Chen, B., Weng, S., Ni, Y.Q., Xu, Y.L., 2012. Temperature effect on vibration properties of civil structures: a literature review and case studies. *J. of Civil Struct. Health Monit.*, **2**(1), 29-46.
- Overschee, V., De Moor, B., 1996. *Subspace identification for linear systems*. Kluwer Academic Publishers, Leuven, Belgio.
- Dohler, E., Reynders, F., Magalhaes, et al., 2010. Pre- and Post - identification Merging for Multi-Setup OMA with Covariance-Driven SSI. *Dynamics of Bridges*, **5**, 55-70.